Available online at www.sciencedirect.com
SCIENCE DIRECT®
Optics Communications 223 (2003) 39–45
OPTICS COMMUNICATIONS
www.elsevier.com/locate/optcom

Perfectly matched layer absorbing boundary conditions in rigorous vector analysis of axially symmetric diffractive optical elements

Yuling Liu*, Zhenwu Lu, Zhibin Ren, Fenyou Li, Zhaoliang Cao

State Key Laboratory of Applied Optics, Changchun Institute of Optics, Fine Mechanics and Physics, Chinese Academy of Sciences, Changchun 13002, China

Received 23 January 2003; received in revised form 16 April 2003; accepted 5 June 2003

Abstract

We extended Berenger's split-field perfectly matched layer (PML) absorbing boundary conditions (ABCs) to cylindrical coordinates for the use in body-of-revolution finite-difference time-domain (BOR FDTD) method that is suitable for the analysis of axially symmetric subwavelength diffractive optical elements (SWDOE). As application, we use our algorithm in the analysis of a multilevel microlens and its counterpart of binary SWDOE. Numerical results illustrate the efficiency of our PML ABCs.
© 2003 Elsevier B.V. All rights reserved.

PACS: 42.79.−e; 02.70.Bf

1. Introduction

Body-of-revolutionary finite-difference time-domain (BOR FDTD) method is suitable for the analysis of axially symmetric subwavelength diffractive optical elements (SWDOE) [1,3]. One of the key issues in the application of the technique is that absorbing boundary conditions (ABCs) must be used to truncate the computational region and absorb outgoing waves, and the accuracy and stability of BOR FDTD code are sensitive to the ABCs that one used. Perfectly matched layer (PML) ABC is popular for its precision [2]. The original PML ABC is presented only in two-dimensional rectangular coordinates. However, for the use of PML ABCs in BOR FDTD, one must extend it to cylindrical coordinates. Some investigators have done it using non-split-field PML method [5,6], and Prather [3] employed their method in the analysis of axially symmetric SWDOE. In this paper, we also extend PML ABCs to cylindrical coordinates for the use in BOR FDTD to analyze axially symmetric SWDOE. However, we presented an alternate method in which we use split-field instead of non-split-field form.

In this paper, we deduced the formulas for the field subcomponents in the PML medium and at

* Corresponding author.
E-mail address: lucy1971lyl@yahoo.com.cn (Y. Liu).

0030-4018/03/$ - see front matter © 2003 Elsevier B.V. All rights reserved.
doi:10.1016/S0030-4018(03)01642-0

the interface for the use in BOR FDTD that is suitable in the analysis of axially symmetric SWDOE. The technique to determine the impedance of PML medium is also presented. As application, we use our PML ABCs in the analysis of a multilevel microlens and its counterpart of binary SWDOE. Numerical results illustrate the utility of our PML ABCs.

2. Perfectly matched layer absorbing boundary conditions

In this section, we extend PML ABCs to BOR FDTD that is suitable for the analysis of axially symmetric SWDOE. We deduce the formulas that are in the PML medium and at the interface of PML and inner computational field. The technique to determine the impedance of the PML medium is also introduced.

2.1. Formulas for the field subcomponents that are in the PML medium

The appropriate starting point for the derivation of formulas is Maxwell's time-depended curl equations with magnetic conductivity

$$\begin{aligned} \nabla \times \vec{E} &= -\mu_0 \frac{\partial \vec{H}}{\partial \vec{t}} - \sigma^* \vec{H}, \\ \nabla \times \vec{H} &= \varepsilon_0 \frac{\partial \vec{E}}{\partial \vec{t}} + \sigma \vec{E}. \end{aligned} \tag{1}$$

The vector $\nabla \times \vec{A}$ in cylindrical coordinates can be expressed as follows:

$$\begin{aligned} \nabla \times \vec{A} = \hat{\vec{r}}\left(\frac{1}{r}\frac{\partial A_z}{\partial \phi} - \frac{\partial A_\phi}{\partial z}\right) + \hat{\vec{\phi}}\left(\frac{\partial A_r}{\partial z} - \frac{\partial A_z}{\partial r}\right) \\ + \hat{\vec{z}}\left(\frac{1}{r}\frac{\partial (rA_\phi)}{\partial r} - \frac{1}{r}\frac{\partial A_r}{\partial \phi}\right). \end{aligned} \tag{2}$$

In this paper, we employ the BOR FDTD method for the analysis of axially symmetric SWDOE in cylindrical coordinates; in this case, one can conveniently orient field polarization in the (ρ–z) plane, which renders the field components of $\vec{E}_r$, $\vec{E}_z$, $\vec{H}_\phi$ as even functions of ϕ and $\vec{H}_r$, $\vec{H}_z$, $\vec{E}_\phi$ as odd functions [3] with the further reason of the value of each electric- and magnetic-field component being periodic in the azimuthal direction, we can expand each field component in Fourier series as follows:

$$\vec{E}_r(r,\phi,z,t) = \sum_{m=0}^{\infty} \vec{E}_r(r,z,t)\cos m\phi, \tag{3a}$$

$$\vec{E}_z(r,\phi,z,t) = \sum_{m=0}^{\infty} \vec{E}_z(r,z,t)\cos m\phi, \tag{3b}$$

$$\vec{E}_\phi(r,\phi,z,t) = \sum_{m=0}^{\infty} \vec{E}_\phi(r,z,t)\sin m\phi, \tag{3c}$$

$$\vec{H}_r(r,\phi,z,t) = \sum_{m=0}^{\infty} \vec{H}_r(r,z,t)\sin m\phi, \tag{3d}$$

$$\vec{H}_z(r,\phi,z,t) = \sum_{m=0}^{\infty} \vec{H}_z(r,z,t)\sin m\phi, \tag{3e}$$

$$\vec{H}_\phi(r,\phi,z,t) = \sum_{m=0}^{\infty} \vec{H}_\phi(r,z,t)\cos m\phi. \tag{3f}$$

By substituting Eq. (2) into Eq. (1), we can obtain six scalar equations. After enforcing Eqs. (3a)–(3f) in the six scalar equations, we can make each field component without variable of ϕ. According to the definition of the PML medium, we can split one field component into two subcomponents, so the six field components of $\vec{E}_r$, $\vec{E}_\phi$, $\vec{E}_z$, $\vec{H}_r$, $\vec{H}_\phi$, and $\vec{H}_z$ can be split into 12 subcomponents correspondingly, 12 scalar equations are generated, which can be expressed as follows:

$$\varepsilon_0 \frac{\partial E_{r\phi}}{\partial t} + \sigma_\phi E_{r\phi} = \frac{m}{r}(H_{zr} + H_{z\phi}), \tag{4a}$$

$$\varepsilon_0 \frac{\partial E_{rz}}{\partial t} + \sigma_z E_{rz} = -\frac{\partial (H_{\phi r} + H_{\phi z})}{\partial z}, \tag{4b}$$

$$\varepsilon_0 \frac{\partial E_{\phi r}}{\partial t} + \sigma_r E_{\phi r} = -\frac{\partial (H_{zr} + H_{z\phi})}{\partial r}, \tag{4c}$$

$$\varepsilon_0 \frac{\partial E_{\phi z}}{\partial t} + \sigma_z E_{\phi z} = \frac{\partial (H_{r\phi} + H_{rz})}{\partial z}, \tag{4d}$$

$$\varepsilon_0 \frac{\partial E_{zr}}{\partial t} + \sigma_r E_{zr} = \frac{1}{r}\frac{\partial [r(H_{\phi r} + H_{\phi z})]}{\partial r}, \tag{4e}$$

$$\varepsilon_0 \frac{\partial E_{z\phi}}{\partial t} + \sigma_\phi E_{z\phi} = -\frac{m}{r}(H_{r\phi} + H_{rz}), \tag{4f}$$

$$\mu_0 \frac{\partial H_{r\phi}}{\partial t} + \sigma_\phi^* H_{r\phi} = \frac{m}{r}(E_{zr} + E_{z\phi}), \tag{4g}$$

$$\mu_0 \frac{\partial h_{rz}}{\partial t} + \sigma_z^* H_{rz} = \frac{\partial(E_{\phi r} + E_{\phi z})}{\partial z}, \tag{4h}$$

$$\mu_0 \frac{\partial H_{\phi r}}{\partial t} + \sigma_r^* H_{\phi r} = \frac{\partial(E_{zr} + E_{z\phi})}{\partial r}, \tag{4i}$$

$$\mu_0 \frac{\partial H_{\phi z}}{\partial t} + \sigma_z^* H_{\phi z} = -\frac{\partial(E_{r\phi} + E_{rz})}{\partial z}, \tag{4j}$$

$$\mu_0 \frac{\partial H_{zr}}{\partial t} + \sigma_r^* H_{zr} = -\frac{1}{r}\frac{\partial[r(E_{\phi r} + E_{\phi z})]}{\partial r}, \tag{4k}$$

$$\mu_0 \frac{\partial H_{z\phi}}{\partial t} + \sigma_\phi^* H_{z\phi} = -\frac{m}{r}(E_{r\phi} + E_{rz}). \tag{4l}$$

Since each field component is not dependent on ϕ, namely, the azimuthal field variation is analytical, we do not need to truncate the grid of FDTD by the PML medium for the ϕ direction, so $\sigma_\phi = \sigma_\phi^* = 0$ and the three-dimensional problems are reduced to two-dimensional problems. Furthermore, since the Z-axis is the rotational symmetric axis, no PML medium is needed in the Z-axis too. For the above reasons, we can construct the general frame of the PML technique as in Fig. 1. The computational domain of the FDTD is truncated by the PML mediums that are normal to the Z- or R-axis. The electric- and magnetic-conductivity can be set as in Fig. 1. The matching condition for the PML medium is as follows: $\sigma_z/\varepsilon_0 = \sigma_z^*/\mu_0$, $\sigma_r/\varepsilon_0 = \sigma_r^*/\mu_0$.

We can employ Yee time stepping for the approximation of time derivative, and then the finite-difference scheme for the PML ABCs of Eqs. (4a)–(4l) can be derived. For illustration we provide here the FDTD approximation for the E_{rz} and $H_{\phi z}$ field subcomponents derived from Eqs. (4b) and (4i), respectively, as the following expression:

$$E_{rz}\big|_{i+\frac{1}{2},j+\frac{1}{2}}^{n+\frac{1}{2}} = \frac{2\varepsilon_0 - \sigma_z\Delta t}{2\varepsilon_0 + \sigma_z\Delta t} E_{rz}\big|_{i+\frac{1}{2},j+\frac{1}{2}}^{n-\frac{1}{2}} - \frac{2\Delta t}{\Delta z(2\varepsilon_0 + \sigma_z\Delta t)} \times \left[H_{\phi r}\big|_{i+\frac{1}{2},j+1}^{n} + H_{\phi z}\big|_{i+\frac{1}{2},j+1}^{n} - H_{\phi r}\big|_{i+\frac{1}{2},j-1}^{n} - H_{\phi z}\big|_{i+\frac{1}{2},j-1}^{n}\right], \tag{5}$$

$$H_{\phi r}\big|_{i+\frac{1}{2},j}^{n+1} = \frac{2\mu_0 - \sigma^*\Delta t}{2\mu_0 + \sigma^*\Delta t} H_{\phi r}\big|_{i+\frac{1}{2},j}^{n-1} + \frac{2\Delta t}{\Delta r(2\mu_0 + \sigma^*\Delta t)} \times \left[E_{zr}\big|_{i+1,j}^{n+\frac{1}{2}} + E_{z\phi}\big|_{i+1,j}^{n+\frac{1}{2}} - E_{zr}\big|_{i,j}^{n+\frac{1}{2}} - E_{z\phi}\big|_{i,j}^{n+\frac{1}{2}}\right]. \tag{6}$$

2.2. Formulas for the field subcomponents at interface

Because the algorithm used in the PML medium and the algorithm used in inner computational domain are different, the formulas for the field subcomponents at the interface must be revised. In

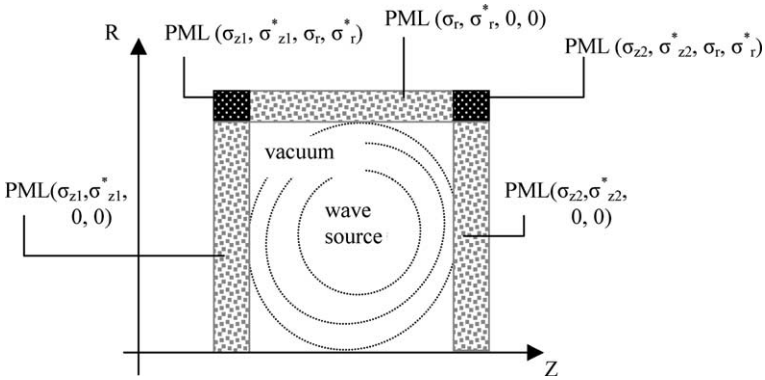

Fig. 1. The PML technique in cylindrical coordinates for the analysis of axially symmetric SWDOE.

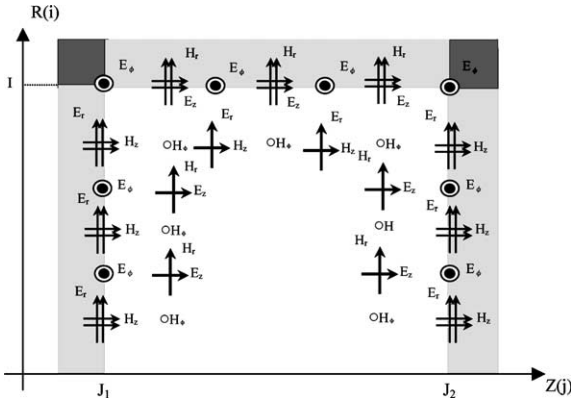

Fig. 2. The distribution of electromagnetic field at the interface.

this paper, we let the incident wave to be normally incident plane wave in the analysis of axially symmetric SWDOE, for this case, all the field components on the Z-axis are zero [3]. We assume that the electric- and magnetic-field components and subcomponents at the interface are distributed as in Fig. 2.

As in Fig. 2 the formulas for the field subcomponents at the interface of $j = J_1$, $j = J_2$, and $i = I$ need to be revised. For example, the electric subcomponent E_{rz} at $j = J_1$, $i = 0, \ldots, I-1$ can be revised as follows

$$E_{rz}\big|_{i+\frac{1}{2},j+\frac{1}{2}}^{n+\frac{1}{2}} = \frac{2\varepsilon_0 - \sigma_z\Delta t}{2\varepsilon_0 + \sigma_z\Delta t} E_{rz}\big|_{i+\frac{1}{2},j+\frac{1}{2}}^{n-\frac{1}{2}} - \frac{2\Delta t}{\Delta z(2\varepsilon_0 + \sigma_z\Delta t)} \times \left[H_\phi\big|_{i+\frac{1}{2},j+1}^{n} - H_{\phi r}\big|_{i+\frac{1}{2},j}^{n} - H_{\phi z}\big|_{i+\frac{1}{2},j}^{n} \right]. \tag{7}$$

The other formulas of subcomponents at the interface can be revised like (7).

2.3. Electric- and magnetic-conductivity in the PML medium

At first the outgoing waves cross the PML medium without reflection for any frequency and incident angle, then totally reflected at the end of PML, after a second crossing, the waves return to the inner domain. Although no reflection occurred for the two times crossing, the magnitude of wave decreases. User can dominate the degree of the decrease, so the reflection factor can be dominated. The reflection factor is [2]

$$R(\theta) = \exp\left(-2\left(\frac{\cos\theta}{\varepsilon_0 c}\right) \int_0^\delta \sigma(\rho)\,\mathrm{d}\rho \right), \tag{8}$$

where θ is the angle of incident radiation relative to the normal direction of the PML surface. $\sigma(\rho)$ the conductivity in the PML whose thickness is δ can be calculated as

$$\sigma(\rho) = \sigma_{\mathrm{m}}\left(\frac{\rho}{\delta}\right)^n, \tag{9}$$

where σ_{m} is the maximum conductivity at the outer side of the PML medium and the user can select $n = 1, 2, 3, \ldots$ By substituting (9) into (8), one can get rid of the integral on the exponent. For normal incidence the reflection factor will be

$$R(0) = \mathrm{e}^{-(2/(n+1))(\sigma_{\mathrm{m}}\delta/\varepsilon_0 c)}. \tag{10}$$

From (10) we can get the maximum conductivity σ_{m}:

$$\sigma_{\mathrm{m}} = \frac{(n+1)c\varepsilon_0}{2\delta} \ln[R(0)^{-1}], \tag{11}$$

where $R(0)$ is a user-defined parameter. After σ_{m} is confirmed, the conductivities in other locations of PML medium can be solved by Eq. (9). However, we also use Yee's grids to solve the EM field in the PML region, and the conductivities in grids can be calculated as follows (for instance, in the r-direction)

$$\sigma_r(i) = \frac{1}{\Delta r} \int_{(i-\frac{1}{2})\Delta r}^{(i+\frac{1}{2})\Delta r} \sigma_{\mathrm{m}}\left(\frac{r}{\delta}\right)^n \mathrm{d}r, \tag{12}$$

where i is the coordinate position and Δr is the space step in the r-direction.

3. Application

As stated above, the outgoing waves from inner domain will be reflected at the end of the PML medium, the number of reflections from PML will increase along with the increase of time steps and if the reflection phenomenon cannot be neglected, the electromagnetic field in the inner domain will not achieve steady state. Actually in a computing

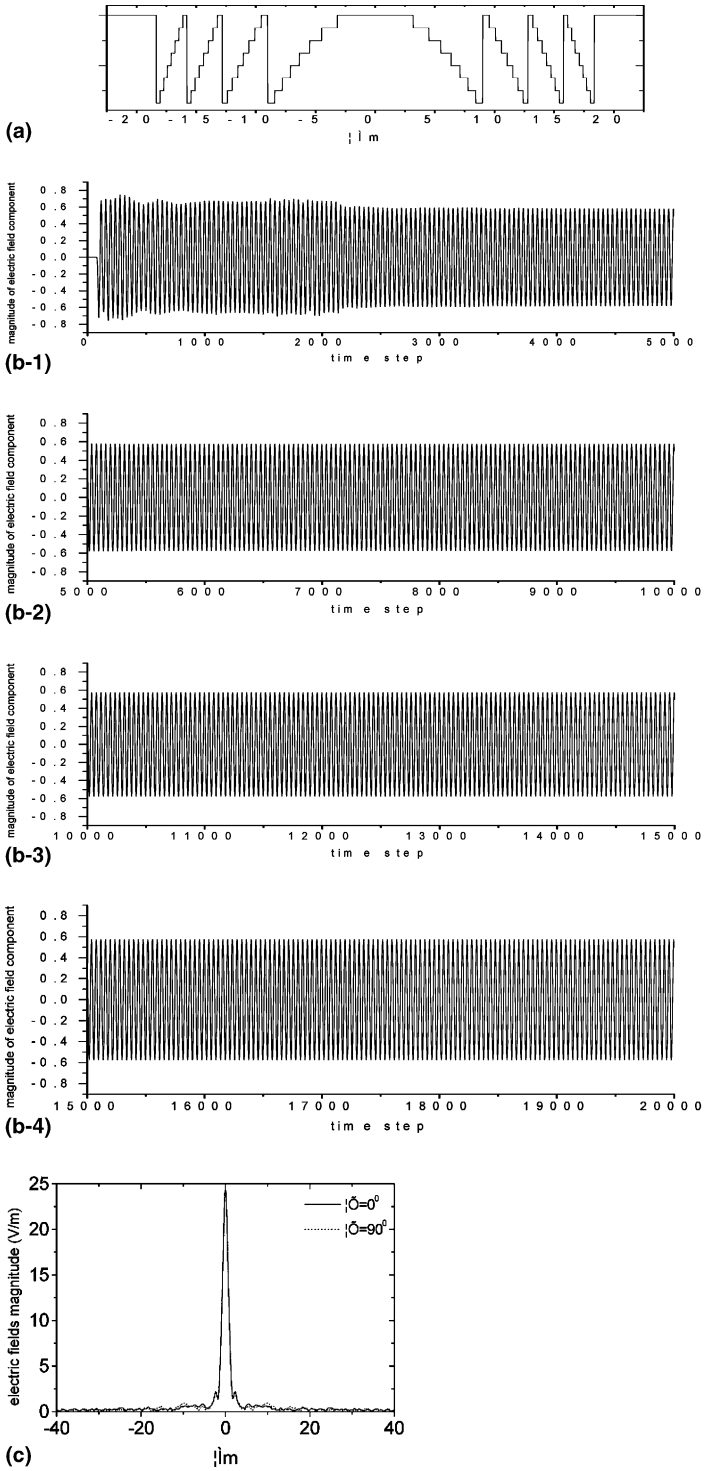

Fig. 3. Illustration of (a) lens profile; (b-1)–(b-4) time-dependent electric-field E_ϕ in FDTD mesh to show steady state; (c) a line scan of the electric-field magnitude in the focal plane of the microlens.

process one can judge the steady state by the vibration curve of the electric-field component. In this paper, we apply the BOR FDTD method with our PML ABC algorithm to the analysis of axially symmetric SWDOE. In our BOR FDTD Matlab code, we let the PML thickness to be 8 cells, conductivity's increasing exponential n to be 2, and the normal incident reflection factor $R(0)$ to be 0.001%. We achieve steady state successfully when we implement our PML technique in code. However, we can only get near field distribution by use of BOR FDTD, and to obtain far field distribution, such as electric-field distribution in the focal plane of SWDOE, we must use the field propagation algorithm. In this paper, we employ the vector-based plane-wave spectrum (VPWS) method [4] to realize near-to-far field transformation.

As application, we analyzed a multilevel microlens same with that in the reference [4] and its counterpart of binary SWDOE [7]. The two elements have the same following parameters: the focal length is 40 μm, the diameter is 36.66 μm, and the index of refraction is 1.5. The incident wave is normal incident plane wave with E_x polarization and the wavelength is 1.0 μm. The microlens is 8-level and 4-zone and shown in Fig. 3(a). In the FDTD working domain, we set the lattice space increments Δr and Δz to be $\lambda/20$ (λ is wavelength) and time increment Δt to be $\Delta r/(2c)$ (c is light speed in vacuum). To illustrate the steady state we run our code for 20,000 time steps and the vibration curve of electric-field component E_ϕ is shown. Due to the large time steps the whole figure is too compressed to distinguish, so we separated it into four parts, which are shown from Figs. 3(b-1) to (b-4). Assuming that waves reflect in the diagonal direction, which is the maximal distance in the working domain, the number of reflections from PML will exceed 25. We also tested our code for 500,000 time steps and we can achieve steady state successfully. Fig. 3(c) shows the magnitude of electric field in the focal plane. It took only 186 s on a 1500-MHz PC to obtain the numerical result. The numerical result is the same with that in the reference [4]. Fig. 4(a) shows the binary SWDOE profile, which is the counterpart of the microlens. Fig. 4(b) illustrates the electric-field magnitude in the focal plane of the binary SWDOE.

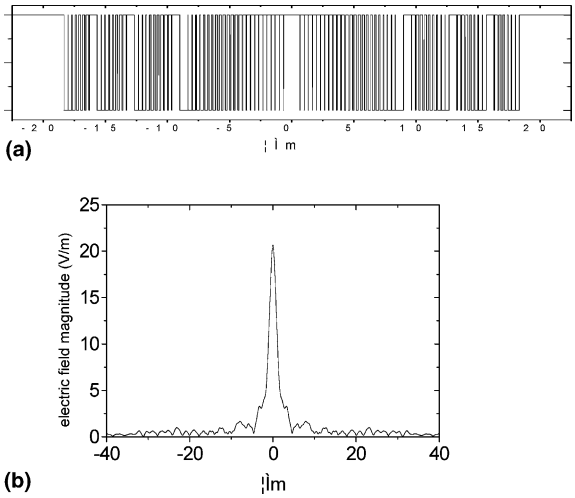

Fig. 4. Illustration of (a) binary SWDOE profile; (b) a line scan of the electric-field magnitude in the focal plane of the binary SWDOE.

4. Summary

We extend Berenger's split-field PML ABCs to cylindrical coordinates for the use in BOR FDTD to analyze axially symmetric SWDOE. We deduced the formulas for the field subcomponents in the PML medium and at the interface. The technique to determine the impedance of PML medium is also presented. We showed the efficiency of the algorithm by applying it to the analysis of a multilevel microlens and its counterpart of binary SWDOE.

References

[1] D. Davidson, R. Ziokowski, J. Opt. Soc. Am. A 11 (1994) 1471.
[2] J.P. Berenger, J. Comput. Phys. 114 (1994) 185.
[3] Dennis W. Prather, Shouyuan Shi, J. Opt. Soc. Am. A 16 (1999) 1131.
[4] Shouyuan Shi, Dennis W. Prather, Opt. Lett. 24 (1999) 1445.
[5] F.L. Teixeira, W.C. Chew, IEEE Microwave Guided Wave Lett. 7 (1997) 285.

[6] Allen Taflove, Susan C. Hagness, Computational Electrodynamics: The Finite-Difference Time-Domain Method, Artech House, Boston, London, 2000, 549–560.

[7] Joseph N. Mait, Dennis W. Prather, Mark S. Mirotznik, Opt. Lett. 23 (1998) 1343.